

## Water balance in hydrological basins. An application based on Google Earth Engine

Ignacio Sánchez-Cohen<sup>1,§</sup>

Sergio Iván Jiménez-Jiménez<sup>1</sup>

Marco Antonio Inzunza-Ibarra<sup>1</sup>

Gabriel Díaz-Padilla<sup>2</sup>

Rafael Alberto Guajardo-Panes<sup>2</sup>

Josué Delgado-Balbuena<sup>3</sup>

1 Centro Nacional de Investigación Disciplinaria en Relación Agua, Suelo, Planta y Atmósfera-INIFAP. Canal Sacramento km 6.5, Zona Industrial, Gómez Palacio, Durango, México. CP. 3140.

2 Campo Experimental Cotaxtla-INIFAP. Carretera Veracruz-Córdoba km 34.5, Medellín de Bravo, Veracruz, México. CP. 94279.

3 Centro Nacional de Investigación Disciplinaria en Agricultura Familiar. Carretera Ojuelos-Lagos de Moreno km 8.5, Jalisco, México. CP. 47540.

Autor para correspondencia: [sanchez.ignacio@inifap.gob.mx](mailto:sanchez.ignacio@inifap.gob.mx).

### Abstract

Within the decision-making process in basins, the water balance requires readily available information and decision tools to accelerate courses of action. The rational starting point in basins is the water balance since it quantifies the basin's potential to produce runoff. Most climate and hydrological information is dispersed and in many formats, which makes the process of analyzing the water balance more difficult and slower. The present code, written in JavaScript, was developed during 2024-2025, in the context of a fiscal project of the National Institute of Forestry, Agricultural and Livestock Research. The ACUAC is designed for use on the Google Earth Engine platform and is focused on hydrological analysis using various data sources. It allows the user to visualize and calculate the water balance for the selected basin based on precipitation, evapotranspiration, and runoff data. The results are presented as graphs and tables, which can be downloaded or edited. The user-friendly interface makes it easy to use and it is very intuitive.

### Keywords:

Google Earth Engine, Water balance, Watersheds, Water resources.



## Introduction

Water is a crucial element for life that defines human wellbeing. In the face of climatic vicissitudes driven by human actions, the uncertainty in water availability is increasingly notorious, as evidenced by the situation of reservoirs and aquifers in the country and worldwide (Gleick, 2014; UN, 2020). In this situation, the options for mitigating, preventing, and designing courses of action involve knowledge of the water balance of the basins, considering them as the fundamental unit for planning water availability.

The water balance allows us to assess the amount of water available at a given time and basically constitutes the count of what enters and leaves a control point, which is essential for the efficient management of water resources. The variables involved in the water balance include precipitation, evapotranspiration, and surface and groundwater runoff, which, when quantified, offer a comprehensive view of the water cycle in a basin (Lijuan *et al.*, 2011; Rodell *et al.*, 2018).

This work aims to present an approach to calculate the basin's water balance using data from different satellite sources. Through the integration of CHIRPS (precipitation), MODIS (evapotranspiration) and GLDAS (runoff) information, an interactive tool is created on the Google Earth Engine (GEE) platform, which allows calculating and visualizing the monthly water balance values. GEE is a platform that stores and analyzes information distributed across space, allowing the analysis of large volumes of geospatial and satellite data (Schroeder *et al.*, 2014).

Its algorithm is in 'the cloud', with its main advantage being access to a vast collection of satellite images and geospatial data, along with advanced analytical tools to perform modeling processes and as an aid to decision-makers in different aspects of natural resources (Gorelick *et al.*, 2017). The combination of these satellite products has proven to be effective for large-scale water balance quantification, particularly in regions where meteorological stations and field data are limited (Hao *et al.*, 2021; Jiménez *et al.*, 2022; Quintana *et al.*, 2023). Location, surface status, and precipitation are defining aspects of a basin's capacity to produce runoff (Velásquez *et al.*, 2017; Li *et al.*, 2022). Water balance is crucial for environmental management studies, water resources planning, and understanding the impact of climate change on the water systems of the selected regions.

## Materials and methods

### Satellite imagery and databases

CHIRPS (precipitation). UCSB-CHG/CHIRPS/DAILY, it is a collection of daily precipitation imagery based on satellite observations and meteorological station data. The application uses this collection to get daily precipitation data for the selected area. The goal with this data source is to extract the daily precipitation amount (in millimeters) for the selected area and the specified date range.

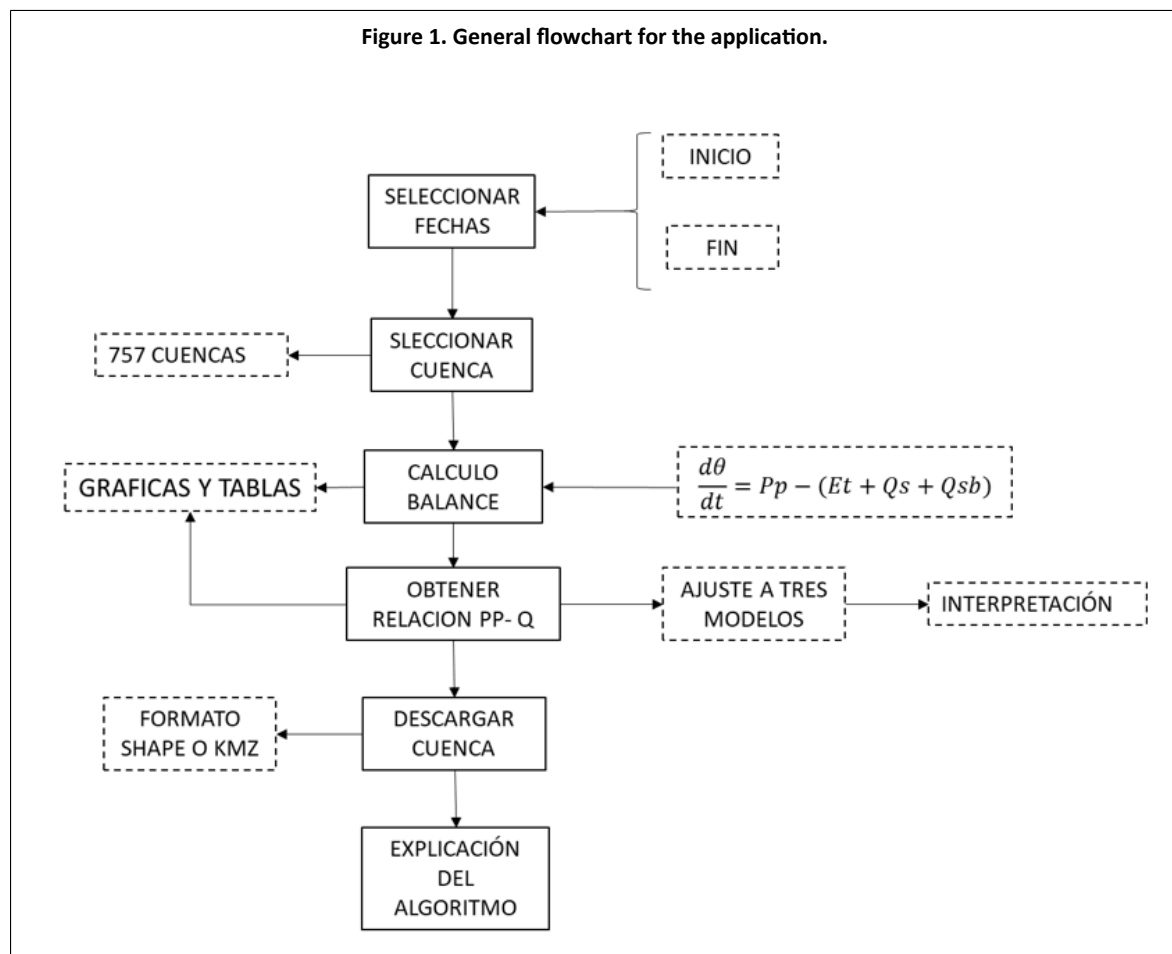
MODIS (evapotranspiration). MODIS/006/MOD16A2, it provides estimates of daily evapotranspiration using the MODIS sensor system from NASA's satellites. The data come from the MOD16A2 product, which has a spatial resolution of 500 m and reports evapotranspiration (ETa) accumulated over eight days.

The NASA/GLDAS/V021/NOAH/G025/T3H dataset is a climate product generated by NASA's Global Land Data Assimilation System (GLDAS) hydrology simulation model, which provides global estimates of hydrological and meteorological variables. This dataset uses the NOAH model to represent physical processes in the atmosphere, land surface, and water, and is available at a spatial resolution of 0.25° (approximately 25 km). The T3H product refers to the version of data at a temporal resolution of 3 h.

### Development of the application in Google Earth Engine (GEE)

The GEE platform provides access to petabytes of public-domain images, as well as high-speed parallel processing and artificial intelligence algorithms using Google's infrastructure (Perilla and

Mas, 2020). It contains programming interfaces compatible with languages such as JavaScript and Python (Jiménez *et al.*, 2022). The general flow diagram of the platform for calculating the water balance in basins is presented in Figure 1.



## The balance model

To define the water balance, expressed as the variation in soil moisture content over time, the following equation was applied:

$$\frac{d\theta}{dt} = Pp - (Et + Qs + Qsb)$$

Where:  $Pp$ = is precipitation;  $Et$ = is the current evapotranspiration;  $Qs$ = is surface runoff; and  $Qsb$ = is subsurface runoff. In equation 1, all variables are in millimeters per month.

## Runoff (Qs)

The numerical models used by GLDAS to calculate surface and subsurface runoff are mainly NOAH, CLM, and VIC, which simulate water flow on the earth's surface by combining assimilated data and balance models. Assimilated data refer to observed data that have been integrated into numerical models to increase their accuracy (Rodell *et al.*, 2004). Thus, the data combine real observations with simulations from models (Kalnay, 2003). Surface runoff (Qs) in these models occurs when precipitation (Pp) exceeds the soil's infiltration capacity (Is). In general, the surface runoff equation can be simplified as:

2)

$$Q = 0 \text{ if } Pp \leq Is; Pp - Is \text{ if } Pp > Is$$

### **Subsurface runoff (Qsb)**

Subsurface runoff (Qsb) refers to water moving into deeper soil layers due to water pressure that exceeds the holding capacity in the surface layer. The equation of Qsb has the following form:

3)

$$Qsb = Ks(\theta - \theta_s)$$

Where Ks (mm hr<sup>-1</sup>) is a constant of proportionality known as hydraulic conductivity that reflects the ability of the soil to conduct water in its matrix when it has been saturated;  $\theta$  (mm) and  $\theta_s$  (mm) are the current soil moisture content and the soil moisture content at saturation, respectively. Equation 1 can be solved for any of its variables, and simplifications can even be made according to the desired objective.

### **Evapotranspiration**

Evapotranspiration is the water balance variable that extracts the most water from the soil and becomes relevant in areas with a low rainfall regime (Allen et al., 1998). In basins, evapotranspiration can be a significant fraction of total precipitation, and in basins with dense vegetation or warm climates, it can be as much as 50% to 80% of annual precipitation.

According to Allan (2000), evapotranspiration in a basin is the physical process that determines the availability of water in the region, and its measurement is essential for the correct management of water resources. The MODIS/006/MOD16A2 model uses an empirical approach to estimate actual evapotranspiration (ETa) from a combination of satellite-based weather and vegetation data.

Potential evapotranspiration (ETo) is one component of this process. The MODIS/006/MOD16A2 data collection, which is used in the application, provides estimates of actual evapotranspiration. The data come from the MOD16A2 product, which has a spatial resolution of 500 m and reports ETa accumulated over eight days. To move from ETo to ETa, the model considers several factors that affect ETa, such as the vegetation index and soil heat flow.

Vegetation index (NDVI): to adjust transpiration based on the density and type of vegetation. Water availability in the soil: under water stress, evapotranspiration is reduced. This is adjusted in the model using coefficients that indicate the limitation of water availability. Surface resistance: it refers to how vegetation and soil or surface prevent water from evaporating, which depends on the type of cover and climatic conditions (Reyes et al., 2019).

Soil heat flux: it is also important for estimating actual evapotranspiration, as the heat absorbed by the surface affects both evaporation and transpiration. Adjustment factor for water availability: MODIS adjusts the ETo to reflect actual soil and vegetation moisture conditions. If water availability is high (in areas with a lot of rainfall or irrigation), the ETa will be close to the ETo, but if water availability is low (in dry areas), the ETa will be lower than the ETo.

### **Validation**

To ensure the good projection of the water balance in any hydrological basin, it is necessary to corroborate the data from the platforms with data measured in the field. In this sense, for the variable 'Eta', data from an Eddy station (Eddy Covariance) located in the experimental area of the National Center for Disciplinary Research in Family Farming of INIFAP were used.

The measurement site has a semi-arid climate with an average annual rainfall of 424 mm and an average annual temperature of 17.5 °C. The topography is dominated by valleys and rolling hills with haplic Xerosols (Delgado *et al.*, 2019). The database consists of a 5-year time series of daily ETa and precipitation information. Data from climatological stations of the National Meteorological Service (SMN), by its Spanish initialism were also available.

Two indices were used for this: Pearson's correlation and Jaccard coefficient. The first was employed to validate the runoff and ETa data, and the second was employed to obtain the degree of similarity in the arrival time (time of occurrence) of the rainfall. Pearson's equation measures the magnitude (positive or negative) of the linear relationship between two continuous variables. The general formula for Pearson's correlation is:

$$4) \quad r = \frac{\sum(x - \bar{x})(y - \bar{y})}{\sqrt{\sum(x - \bar{x})^2 \sum(y - \bar{y})^2}}$$

Where: x and y are the variables to compare. The closer the value is to one, the better the correlation between the variables. As has been established, in terms of precipitation, more important than precipitation quantities in comparison studies is the time of arrival; that is, the time at which rainfall events occur.

For this description, the Jaccard coefficient was used, applying it to the two time series (MODIS and Eddy Tower). The Jaccard coefficient is defined as a measure of similarity between two data series and is expressed as:

$$J_{1,2} = \frac{J_1 \cap J_2}{J_1 \cup J_2}$$

Where:  $J_1 \cap J_2$  is the number of common elements in both series and  $J_1 \cup J_2$  are all elements present in at least one of the series. There are different computational packages that analyze this coefficient; an example is the R software (García, 2004).

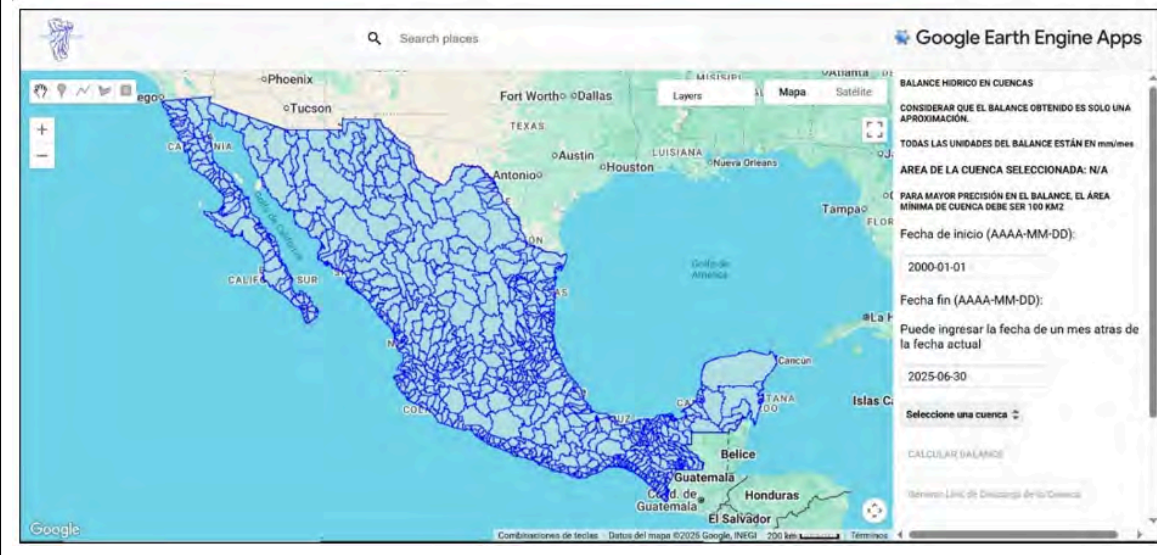
## Results and discussion

### Platform development

Figure 2 shows the application's general interface, which contains a general menu and 'combos' for selecting variables. The user must enter the start and end dates of the water balance. In this sense, considering the timescales of the different data sources, the application proposes the dates that appear by default in the console.



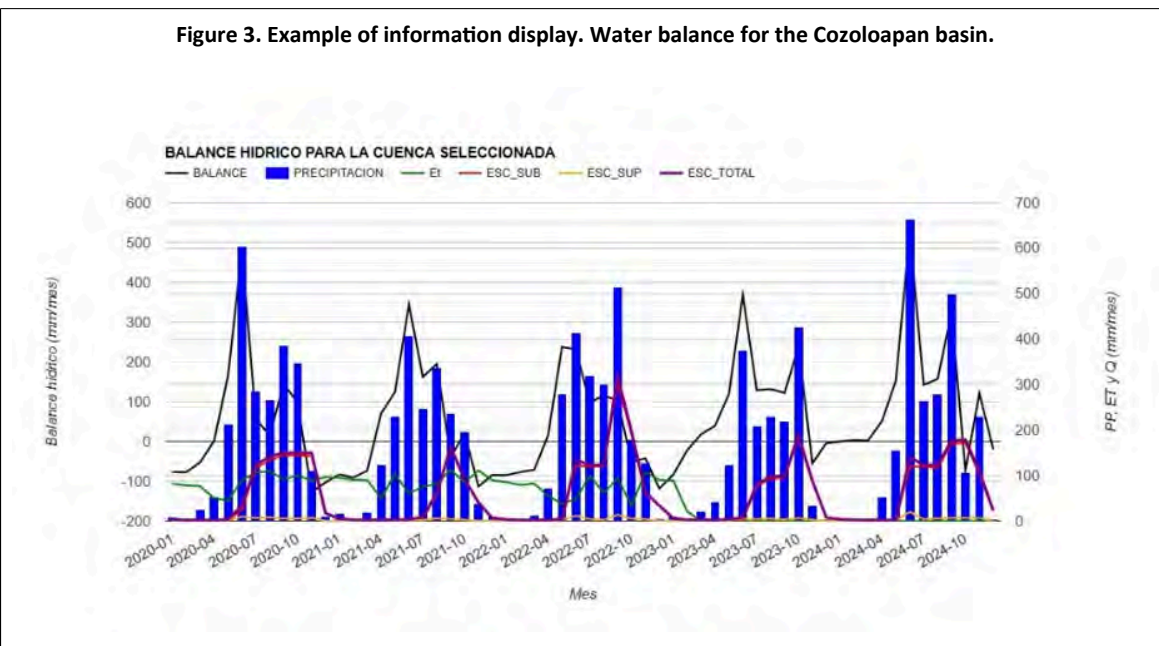
**Figure 2. General interface of the GEE platform for basin water balance. <https://tatiyoma85.users.earthengine.app/view/balance-hidrico-en-cuenca>.**



This will change as the sources of information are updated. Nevertheless, the user will be able to choose a sub-range of interest. A basin must also be chosen. The platform includes the 757 basins in which the National Water Commission has discretized the country's hydrology (CNA, 2021).

Once a basin in the combo has been selected, the platform will automatically zoom in on the selected basin. The water balance of the chosen basin will be obtained by pressing the 'calcular balance' button. The output of this balance is in graphical and tabular form (Figure 3). Different basins can be chosen to make comparisons between them in terms of the precipitation-runoff relationship.

**Figure 3. Example of information display. Water balance for the Cozoloapan basin.**



The option for obtaining the precipitation-runoff relationship displays three adjustment models so that the user has a more objective appreciation of the basin's capacities to produce runoff. An interpretation of the adjusted models is also displayed (Figure 4). These models are linear, potential, and exponential. The reason is that runoff behaves differently across the country's different rainfall regimes. Thus, the adjustment will depend on the response of this variable in the different basins.

Figure 4. Precipitation-runoff relationship for the selected basin and interpretation of the best adjustment model.



#### INTERPRETACIÓN DEL MODELO LINEAL:

El modelo lineal ( $Q = 0.3131 \times P - 36.21$ ) indica que por cada milímetro de precipitación, el escurrimiento aumenta en 0.3131 mm. El coeficiente 0.3131 representa el coeficiente de escurrimiento de la cuenca. El valor de intercepción negativo (-36.21) sugiere que una cantidad inicial de precipitación es capturada por el suelo o vegetación antes de que se genere escurrimiento.

#### CALIDAD DEL AJUSTE:

El  $R^2$  entre 0.4 y 0.6 indica una relación moderada. La precipitación explica parcialmente el escurrimiento, pero otros factores como uso de suelo, condiciones de humedad previas o estacionalidad también son importantes.

#### IMPlicaciones para la Gestión Hídrica:

El comportamiento lineal facilita la predicción y planificación de recursos hídricos. El coeficiente de escurrimiento (0.3131) puede utilizarse para estimar volúmenes de escurrimiento a partir de pronósticos de precipitación.

**X Cerrar**

The user can download the file of the chosen basin in Shape format for use in a geographic information system or KML format for visualization in Google Earth.

## Validation

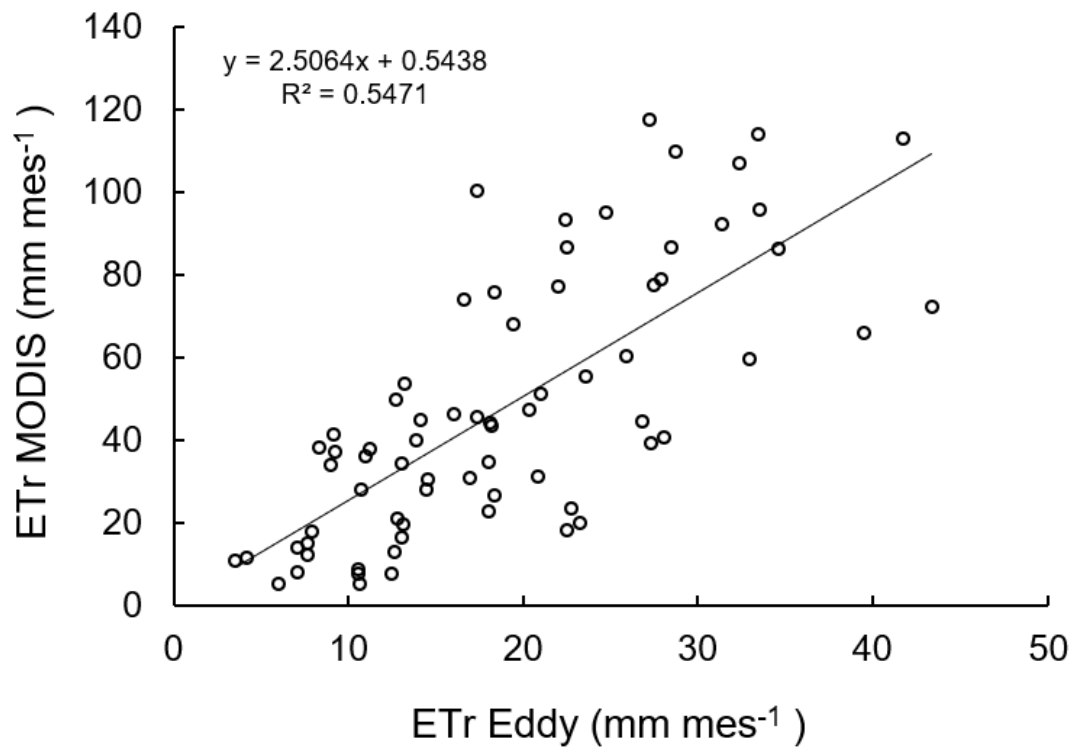
In the present case, the Jaccard coefficient for precipitation yielded a value of 0.5, indicating that there is a 50% similarity in the time of occurrence of precipitation, which is considered acceptable given the different sources and scales of the time series compared (Real and Vargas, 1996).

As for the similarity between the evapotranspiration data from the MODIS satellite and the data measured with an Eddy Covariance tower, Pearson's coefficient yields a value of 0.65. Studies conducted by Zhang *et al.* (2015) obtained similar results when comparing water use efficiency, where evapotranspiration plays a preponderant role, with the Eddy tower having obtained a Pearson coefficient of 0.6 to 0.8.

It should be clarified, as mentioned by Delgado *et al.* (2019), that the tower was installed in a pasture in a semi-arid region; however, the foot print (area of influence in the measurements) exceeds the limits of the pasture area, involving native vegetation of the region, which strengthens the similarity with the evapotranspiration data of the MODIS satellite (Figure 5).

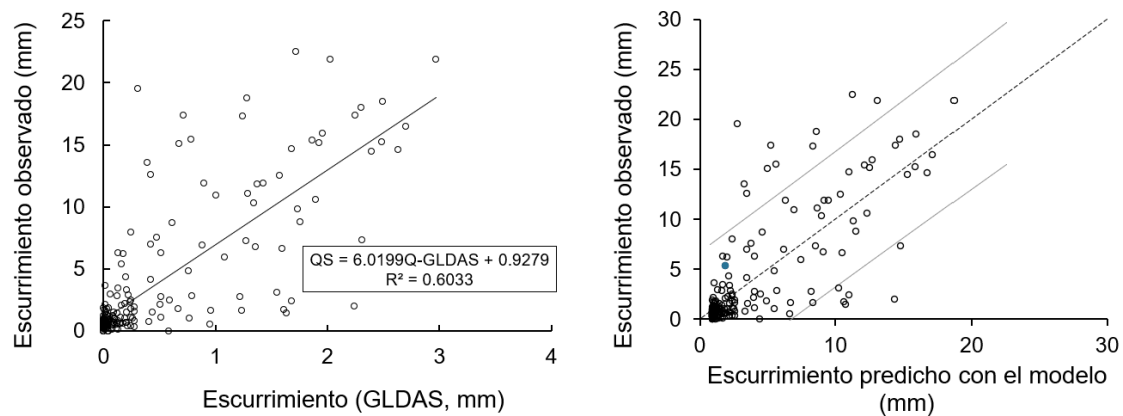


**Figure 5. Relationship between actual evapotranspiration (ET<sub>a</sub>) data measured with the Eddy Covariance flux tower and data from the MODIS system.**



Regarding runoff, data on this variable measured in one of the Yaqui River basins (Yaqui River 1) were used. The reanalysis data explain 60% of the variability in runoff (Figure 6).

**Figure 6. For runoff, GLDAS data explain 60% of the variability of the dependent variable (Yaqui River Basin 1). Right, predictive capacity of the model.**



Zhao *et al.* (2015) obtained similar results across different basins in China, where they compared observed runoff data with GLDA-derived simulations, evaluating its applicability for hydrological modeling.

## Conclusions

The balance hídrico en cuencas application is a comprehensive tool for hydrological analysis in basins using Google Earth Engine. It integrates various sources of information effectively, in addition to providing a user-friendly interface. It allows an analysis of the components of the hydrological balance and the precipitation-runoff relationship, where three regression models are analyzed: linear, exponential, and potential, choosing the one with the best fit and explaining the meaning of its parameters. The application provides options to download the basin information and explains the calculations.

## Bibliography

- 1 Allan, J. A. 2000. Virtual water: A strategic resource in international food policy and water policy. *International Journal of Water Resources Development*. 15(1):61-75.
- 2 Allen, R. G.; Pereira, L. S.; Raes, D. and Smith, M. 1998. Crop evapotranspiration: Guidelines for computing crop water requirements FAO Irrigation and Drainage Paper No. 56. Food and Agriculture Organization of the United Nations (FAO). 3-13 pp. <http://www.fao.org/3/X0490E/x0490e00.html>.
- 3 CNA. 2021. Estadísticas del agua en México. 42-52 pp. <https://files.conagua.gob.mx/conagua/publicaciones/Publicaciones/EAM%202021.pdf>.
- 4 Delgado, B. J.; Arredondo, J. T.; Loescher, H. W.; Pineda-Martínez, L. F.; Carbajal, J. N. and Vargas, R. 2019. Seasonal precipitation legacy effects determine the carbon balance of a semiarid grassland. *Journal of Geophysical Research: biogeosciences*. 124(4):987-1000. <https://doi.org/10.1029/2018JG004799>.
- 5 García-Codron, J. C.; Diego-Liaño, C.; Fdez-Arróyabe, H. P.; Garmendia-Pedraja, C. y Rasilla Álvarez, D. 2004. El clima entre el mar y la montaña. Asociación Española de Climatología y Universidad de Cantabria. 619-628 pp.
- 6 Gleick, P. H. 2014. Water security: The water-food-energy-climate nexus. *Science*. 345(6198):318-322. <https://doi.org/10.1126/science.1258852>.
- 7 Gorelick, N.; Hancher, M.; Dixon, M.; Ilyushchenko, S.; Thau, D. and Moore, R. 2017. Google earth engine: planetary-scale geospatial analysis for everyone. *Remote Sensing of Environment*. 202(1):18-27. <https://doi.org/10.1016/j.rse.2017.06.031>.
- 8 Hao, Z.; Chen, X. and Zhang, X. 2021. Satellite-based hydrological modeling and water resource management. *Remote Sensing*. 13(12):2423. <https://doi.org/10.3390/rs13122423>.
- 9 Jiménez-Jiménez, S.; Marcial, P. M. J.; Ojeda, B. W.; Sifuentes, B. E.; Inzunza, M. A. and Sanchez, C. I. 2022. VICAL: global calculator to estimate vegetation indices for agricultural areas with landsat and sentinel-2 Data. *Agronomy*. 12(7):1518. Doi:10.3390/agronomy12071518.
- 10 Kalnay, E. 2003. Atmospheric modeling, data assimilation and predictability. Cambridge University Press. 150-170 pp. <https://assets.cambridge.org/9780521796293-frontmatter/9780521796293-frontmatter.pdf>.
- 11 Li, Y.; Wang, Z. and Zhang, L. 2022. Impact of terrain and land use on hydrological modeling accuracy in large basins using satellite-derived data. *Journal of Hydrology*, 599:126306. <https://doi.org/10.1016/j.jhydrol.2021.126306>.

12 Lijuan, C.; Yong, Z. and Ying, S. 2011. Climate change effect on hydrological processes over the Yangtze River basin. *Quaternary International*. 244(2):202-210 <https://doi.org/10.1016/j.quaint.2011.01.004>.

13 Perilla, G. A. and Mas, J. F. 2020. Google Earth Engine (GEE): una poderosa herramienta que vincula el potencial de los datos masivos y la eficacia del procesamiento en la nube. *Investigaciones Geográficas*, (101). <https://doi.org/10.14350/ig.59929>.

14 Quintana-Molina, J. R.; Sánchez-Cohen, I.; Jiménez-Jiménez, S. I.; Marcial-Pablo, M. J.; Trejo-Calzada, R. and Quintana-Molina, E. 2023. Calibration of volumetric soil moisture using Landsat-8 and Sentinel-2 satellite imagery by Google Earth Engine. *Revista de Teledetección*. 62:21-38. <https://doi.org/10.4995/raet.2023.19368>.

15 Real, R. and Vargas, J. M. 1996. The probabilistic basis of Jaccard's index of similarity. *Systematic Biology*. 45(3):380-385. <https://doi.org/10.1093/sysbio/45.3.380>.

16 Reyes, J.; Pérez, M. y Rodríguez, L. 2019. Modelamiento de evapotranspiración en cultivo utilizando índices de vegetación obtenidos con sensores remotos Sentinel-2: Caso de estudio desarrollado en CENICAÑA 2019-2020. 83 p.

17 Rodell, M.; Velicogna, I. and Famiglietti, J. S. 2018. Satellite-based estimates of groundwater depletion in India. *Nature*. 460(7258):999-1002. <https://doi.org/10.1038/nature08238>.

18 Rodell, M.; Houser, P. R.; Jambor, U.; Gottschalck, J.; Mitchell, K.; Arsenault, K. and Lohmann, D. 2004. The global land data assimilation system. *Bulletin of the American Meteorological Society*. 85 (3):381-394.

19 Schroeder, W.; Sulla-Menashe, D. and Giglio, L. 2014. The MODIS active fire detection algorithm and data products: an overview. *Remote Sensing of Environment*. 178(216):370-380. <https://doi.org/10.1016/j.rse.2013.07.028>.

20 United Nations. 2020. The United Nations world water development report. Water and climate change. UNESCO. 79-94 pp. <https://unesdoc.unesco.org/ark:/48223/pf0000372983>.

21 Velásquez-Valle, M. A.; Sánchez-Cohen, I. and Hawkins, R. H. 2017. Rainfall runoff relationships in a semiarid rangeland watershed in central Mexico based on the CN-NRCS approach. *Model. Earth Syst. Environ.* 3(2):1263-1272. <https://doi.org/10.1007/s40808-017-0379-8>.

22 Zhang, L.; Tian, J. and He, H. 2015. Evaluation of water use efficiency derived from MODIS products against eddy variance measurements in China. *Remote Sensing*. 7(9):11183-11201.

23 Zhao, F.; Tang, Q.; Liu, X. and Zhang, X. 2015. Assessing the performance of remotely sensed precipitation and GLDAS hydrological variables in streamflow simulation in the Huaihe river basin, China. *Hydrology and Earth System Sciences*. 19(5):2201-2213. <https://doi.org/10.5194/hess-19-2201-2015>.

24 Zhang, L.; Liu, D. and Zhou, Y. 2020. Evaluation of remote sensing-based precipitation datasets for hydrological applications. *Journal of Hydrometeorology*. 21(4):919-934. <https://doi.org/10.1175/JHM-D-19-0120.1>.



## Water balance in hydrological basins. An application based on Google Earth Engine

Journal Information
Journal ID (publisher-id): remexca
Title: Revista Mexicana de Ciencias Agrícolas
Abbreviated Title: Rev. Mex. Cienc. Agríc
ISSN (print): 2007-0934
ISSN (electronic): 2007-9934
Publisher: Instituto Nacional de Investigaciones Forestales, Agrícolas y Pecuarias

Article/Issue Information
Date received: 01 November 2025
Date accepted: 01 February 2026
Publication date: 01 January 2026
Publication date: Jan-Feb 2026
Volume: 17
Issue: 1
Electronic Location Identifier: e3890
DOI: 10.29312/remexca.v17i1.3890
Publisher ID: 00006

### Categories

Subject: Article

### Keywords:

#### Keywords:

Google Earth Engine  
Water balance  
Watersheds  
Water resources

### Counts

Figures: 6

Tables: 0

Equations: 5

References: 24